Molecules and Cells

Mineralized Polysaccharide Transplantation Modules Supporting Human MSC Conversion into Osteogenic Cells and Osteoid Tissue in a Non-Union Defect

Qing Ge[1], David William Green[1], Dong-Joon Lee[1], Hyun-Yi Kim[1], Zhengguo Piao[2], Jong-Min Lee[1], and Han-Sung Jung[1,*]

[1]Division in Anatomy and Developmental Biology, Department of Oral Biology, Oral Science Research Center, BK21 PLUS Project, Yonsei University College of Dentistry, Seoul, Korea, [2]Department of Oral and Maxillofacial Surgery, Affiliated Stomatology Hospital of Guangzhou Medical University, Guangzhou, China
*Correspondence: hsjung@yuhs.ac
http://dx.doi.org/10.14348/molcells.2018.1001
www.molcells.org

Regenerative orthopedics needs significant devices to transplant human stem cells into damaged tissue and encourage automatic growth into replacements suitable for the human skeleton. Soft biomaterials have similarities in mechanical, structural and architectural properties to natural extracellular matrix (ECM), but often lack essential ECM molecules and signals. Here we engineer mineralized polysaccharide beads to transform MSCs into osteogenic cells and osteoid tissue for transplantation. Bone morphogenic proteins (BMP-2) and indispensable ECM proteins both directed differentiation inside alginate beads. Laminin and collagen IV basement membrane matrix proteins fixed and organized MSCs onto the alginate matrix, and BMP-2 drove differentiation, osteoid tissue self-assembly, and small-scale mineralization. Augmentation of alginate is necessary, and we showed that a few rationally selected small proteins from the basement membrane (BM) compartment of the ECM were sufficient to up-regulate cell expression of Runx-2 and osteocalcin for osteoid formation, resulting in Alizarin red-positive mineral nodules. More significantly, nested BMP-2 and BM beads added to a non-union skull defect, self-generated osteoid expressing osteopontin (OPN) and osteocalcin (OCN) in a chain along the defect, at only four weeks, establishing a framework for complete regeneration expected in 6 and 12 weeks. Alginate beads are beneficial surgical devices for transplanting therapeutic cells in programmed (by the ECM components and alginate-chitosan properties) reaction environments ideal for promoting bone tissue.

Keywords: alginate encapsulation, growth factor, mesenchymal stem cells, non-union bone defect, osteogenesis

INTRODUCTION

Bone tissue engineering involves the use and development of biomaterials to transplant reparative cells, organize cells and replace the space that was previously occupied by diseased or degenerated tissue (Stevens, 2008). As with all degenerated or diseased tissues in the body, it is the lack of essential populations of cells for large-scale tissue repair that is the root problem (Murry and Keller, 2008). Thus, it is necessary to use cells in sufficient numbers to effectively regenerate and to combat pathology.

Received 28 December 2017; revised 18 July 2018; accepted 23 August 2018; published online 6 November, 2018

eISSN: 0219-1032

Bone tissue engineering currently follows three tracks: use of cells, cells combined with scaffolds and materials alone (Crane et al., 1995; Gong et al., 2015). Tissue engineering according to the compositing and compound strategy between materials and therapeutic cells have the advantage of including physical properties and deputizing for the native ECM, which is not present or disrupted in the donor site. Soft matter made from protein and polysaccharides of synthetic or natural origins are fabricated from first principles and adapted with small molecules (Defined by the correct functional ligands and receptors) to promote, guide and build new tissues or to activate and tightly regulate the behavior of therapeutic cells for various types of clinical treatment. However, many "short ECM-derived ligands" give rise to chemically precision design and assembly into ECM resembling complexity (Collier and Segura, 2011).

Stem cell encapsulation assures the viability and function of stem cells for various therapeutic applications including cancer therapy (Shah, 2013) Embedding stem cells in the hydrogel provides mechanical protection, shields the cells from specific disruptive host cells and places the cells in supportive physical and chemical-based microenvironments that facilitate stem cell behavior under precise control. Many kinds of hydrogel have been evaluated and validated as a framework for stem cell therapy to improve stem cell retention, preserve viability, and target signal molecules onto cell receptors (Burdick et al., 2016). Cell-laden hydrogels are designed for safe and protective transplantation for tissue deputisation and substitution. The primary purpose is to transplant stem cell safely into a specific location of the vacated tissue. A popular and frequently used hydrogel is alginate due to its low cost and easy attainability as well as its wide range of encapsulation functions such as cryoprotection (Swioklo et al., 2016).

Sodium and calcium alginates are a versatile material but must be modified and enhanced with receptors, integrins and, morphogens to control and induce cells to regenerate tissues (Ansari et al., 2014; Augst et al., 2006; Bouhadir et al., 2005; Lee and Mooney, 2012; Luo et al., 2015; 2016; Moshaverinia et al., 2013; Muzzarelli et al., 2015; Perez et al., 2013; Place et al., 2015; Qiao et al., 2015; Rowley et al., 1999; Sajesh et al., 2013; Sowjanya et al., 2013; Venkatesan et al., 2015; Xia et al., 2013). The requirements for clinical use for cartilage regeneration with attached human chondrocytes includes a molecular composition of an alginate linear copolymer that provides for (1,4)-linked β-D mannuronate residues (M-blocks) and α-L-guluronate residues (G-blocks), resorption kinetics that is smoothed by sodium periodate based partial oxidization treatment (Bouhadir et al., 2001), crosslinking with metalloproteinase (MMP)-only labile peptides (Fonseca et al., 2014), crosslinking densities by ions or covalency (Jang et al., 2014), stiffness characteristics that match the corresponding tissues (Mao et al., 2016) and conjugation with adhesive peptides (RGD, YIGSR (Tyr-Ile-Gly-Ser-Arg) and DGEA (Asp-Gly-Glu-Ala)) Alginate has properties that are highly suited to cartilage regeneration (Lee and Mooney, 2012). Besides, its high calcium content is useful to stimulate bone regeneration. Previously alginate hydrogels have been produced into droplets, stabilized by chitosan and infused with human collagen type I polypeptides and rhBMP 2 to accelerate cell activity in favor of osteogenic fates (Pound et al., 2006). The cell stimulating additives should also include small protein molecules, but only with the correct functional domains.

We predicted that the basement membrane foundations, which have been shown to promote cell differentiation in culture and absent in alginate, induce cell self-assembly, leading to tissue fates of a high calcium mineral content plus BMP-2 loading, which accelerates bone tissue formation in alginate capsules. The reason for the existence of basement membrane elements inside the capsule is to increase ligand presentation and to bind with cell receptors. The actual density of basement membrane receptors affects the frequency of corresponding integrins (α6β4) along the cell membrane that is involved in cell fixation (Chaudhuri et al., 2014).

In this study, we designed and fabricated alginate hydrogel based microenvironments for converting human mesenchymal stem cells into committed, osteocalcin and collagen I secreting osteogenic cells with the capacity to deliver bone cells inside safe and protected transplantation beads. Moreover, the 3D bead environments provide a template for bone tissue formation.

MATERIALS AND METHODS

Mesenchymal stem cell culture

Primary human mesenchymal cells (Poietics™ human MSCs, Lonza, Wlakersville. Inc.) were obtained from a commercial source and grown using the proprietary protocol provided by Lonza. Mesenchymal stem cells were cultured at cell seed densities of 2×10^6 - $4 \times 10^6/cm^2$ in Dulbecco's Modified Eagle Medium (DMEM (1X) + GlutaMAX; Gibco; Life Technologies) with 10% FBS and supplemented with penicillin and streptomycin. The growth of hMSCs for seven days preceded encapsulation. A single culture dish of hMSCs after seven days of culture contained 2 million cells at an approximately 95% confluence level. hMSCs were trypsinized and pelleted before the addition of 1 ml of a 5% alginate solution.

Immunohistochemistry for cell phenotype determination

Wax sectioned slices were de-waxed at 60℃ before rehydration through an ethanol series followed by distilled water. Next, the sections were blocked with serum and incubated with various monoclonal antibodies that mark the presence of critical components of osteogenic tissue: (I) Collagen type I, (II) Alkaline phosphatase, (III) Osterix, (IV) Runx-2 (essential for osteoblast differentiation as one of the principal master regulatory genes) and (V) Osteocalcin. Next, we stained embedded cells with a stem cell-specific surface marker to (a) validate that encapsulated cells were phenotypically stem cells and (b) to establish the conversion of hMSCs during culture inside the beads between 7 and 28 days (the standard minimum time for mineralization to occur). Tissue sections were washed gently, to prevent the specimens from detaching, and then incubated with mouse anti-rabbit secondary antibodies (Sigma-Aldrich). Marker expression was examined under a light

microscope at x200 and x400 magnifications, for horseradish peroxidase staining and under a laser confocal microscope compiled from combined TRITC and FITC emissions, at x100 magnifications (LSM-700 Zeiss).

Alginate formulations with biomolecule additives

Nanogram concentrations of human proteins infused with alginate were BMP-2 and different kinds of small BM protein fragments. (Yang et al., 2004). The ECM additives inside the beads were the essential and integral components of the basement membrane complex involved in cell attachment and organization as well as the specific mechanically related cadherins and gene activation pathways, such as, MAPK/ERK, similar to cell proliferation: Human collagen IV polypeptide (0.4 mg/ml = 40 μg per capsule) (from human placenta, Bornstein and Traub Type IV)), laminin (from human fibroblasts) polypeptides with conserved cell functioning domains (0.9 mg/ml = 90 μg per capsule) and chondroitin sulfate proteoglycan (human cartilage; 0.23 mg = 23 μg per capsule). A previous study showed that laminin administered at 100 micrograms affected ESC conversion into neurons (Ma et al., 2008). Conventionally, 20 μg/ml laminin was coated onto the TCP surfaces for active cell induction cultures. Each of the individual components was added, as a solution, and mixed in the alginate solution. The quantity selected was positioned in the range of probability for physiological activity.

Polysaccharide beads fabrication

Synthesis of mineralized alginate/ chitosan beads by a previously described method. Sodium alginate (Novamatrix Pharmaceutical grade) was filter sterilized and used to make the cell suspension. One-mm diameter drops of alginate were added to a solution of sterilized chitosan (MMW), supplemented with 150 mM of sodium phosphate (the phosphate donor for the CaP membrane). The generation of smooth beads was spontaneous, and the needle gauge specified the bead size (22G; O.D. 0.71 mm) from the dispensing syringe. Chitosan was bound in a 2-5 um membrane to the alginate droplet after 30 min (Figs. 1A and 1B(ii)). During that time mineralization began by the precipitation of calcium phosphate.

Polysaccharide bead-in-bead fabrication

Polysaccharide bead-in-bead arrangements were generated according to a previously published method (Green et al., 2005). Chitosan solution prepared sizeable soft alginate beads. Smaller beads were made with BMP-2 and stiffened for 30 min. Small stiff beads were inserted, manually into soft beads one at a time. After Guest bead insertion the alginate was repaired by the chitosan solution. The large beads were then allowed to stiffen as usual.

Alizarin red staining and polarized light microscopy

Thin sections of beads were stained with an Alizarin red solution (3, 4-Dihydroxy-9, 10-dioxo-2-anthracenesulfonic acid sodium salt) to detect of mineralization, and then imaged in polarized light to distinguish crystallization in the matrix synthesized by cells inside the beads.

Cranial defect implantation of beads

Non-union defects created a hole in the top part of the skull, offset on either side from the midline. Defects were 5 mm holes for insertion of three single beads (2 mm in diameter) with a pair of forceps, and the skin flaps were stitched together with silk sutures. In five mice four different kinds of bead were implanted: MSCs alone, MSCs + BMP-2, MSCs + BM and MSCs with a nested BMP-2 bead. After four weeks, the entire skull was dissected out from the dead mice and immediately fixed and processed for decalcification lasting three days.

RESULTS

Mineralised alginate- chitosan bead generation

Generation of scores of mineralized alginate-chitosan beads was achieved using a previously published method (Fig. 1A) (Green et al., 2005). Every bead contained between 500,000-600,000 hMSCs spread evenly following a relatively gentle mixing procedure. The membrane structure is essential for additional stabilization of the alginate core by reducing swelling, and passively controls the permeability of solutes and molecules between the external aqueous environment and the alginate core (Fig. 1B). The alginate droplets were homogenous, and the core volume was confined to 0.524 mm^3 to guarantee diffusivity to cells at the center (Fig. 1C). Cell distribution inside crosslinked beads was even (Fig. 1C(i)). We manufactured two kinds of alginate environment with the proteins, BM and BMP-2, and made a nested bead with BMP-2 (for tighter control of BMP diffusion). Control beads were alginate without the proteins (Fig. 1C).

Cellular structure density and distribution of cells inside of the beads

One-day-old alginate-chitosan beads were fixed, sectioned and stained with hematoxylin and eosin (H & E) and showed that the cells were evenly separated or in loose or tight clusters with variable statistically insignificant calculated density of 12 cells per 50 μm^3 (Figs. 1D and 1E). The hMSCs inside BMP-2 beads, BM beads, and guest BMP-2 beads existed at higher densities than MSC beads in 24-hour cultures (Figs. 1D and 1E). In two-week cultures, the MSC beads maintained 24-hour cell numbers. In contrast, the BMP-2, BM and nested BMP-2 bead cell numbers increased notably from the 24-hour cell counts, as the BMP-2 effects in nanogram quantities are differentiation, a higher proliferation rate, and low apoptosis (Kim et al., 2013)(Figs. 1D and 1E). In Fig. 1E we highlight the changes and differences in cell numbers between beads that develop over 4-week cultures. The result is a consistent cell increase at similar rates but that the nested BMP-2 and BM show much higher numbers overall, at one day, two weeks, three weeks and four weeks. We suggest that the increased retention of BMP-2 inside the nested bead enhances BMP-2 cell function and similarly that BM cell attachment improves proliferation.

In four-week cultures, the BMP-2 beads, BM beads, and the guest BMP-2 beads appeared with a tight, densified structure than the MSC beads. Besides, the alginate developed lacunae around cells caused by maturating cells as they

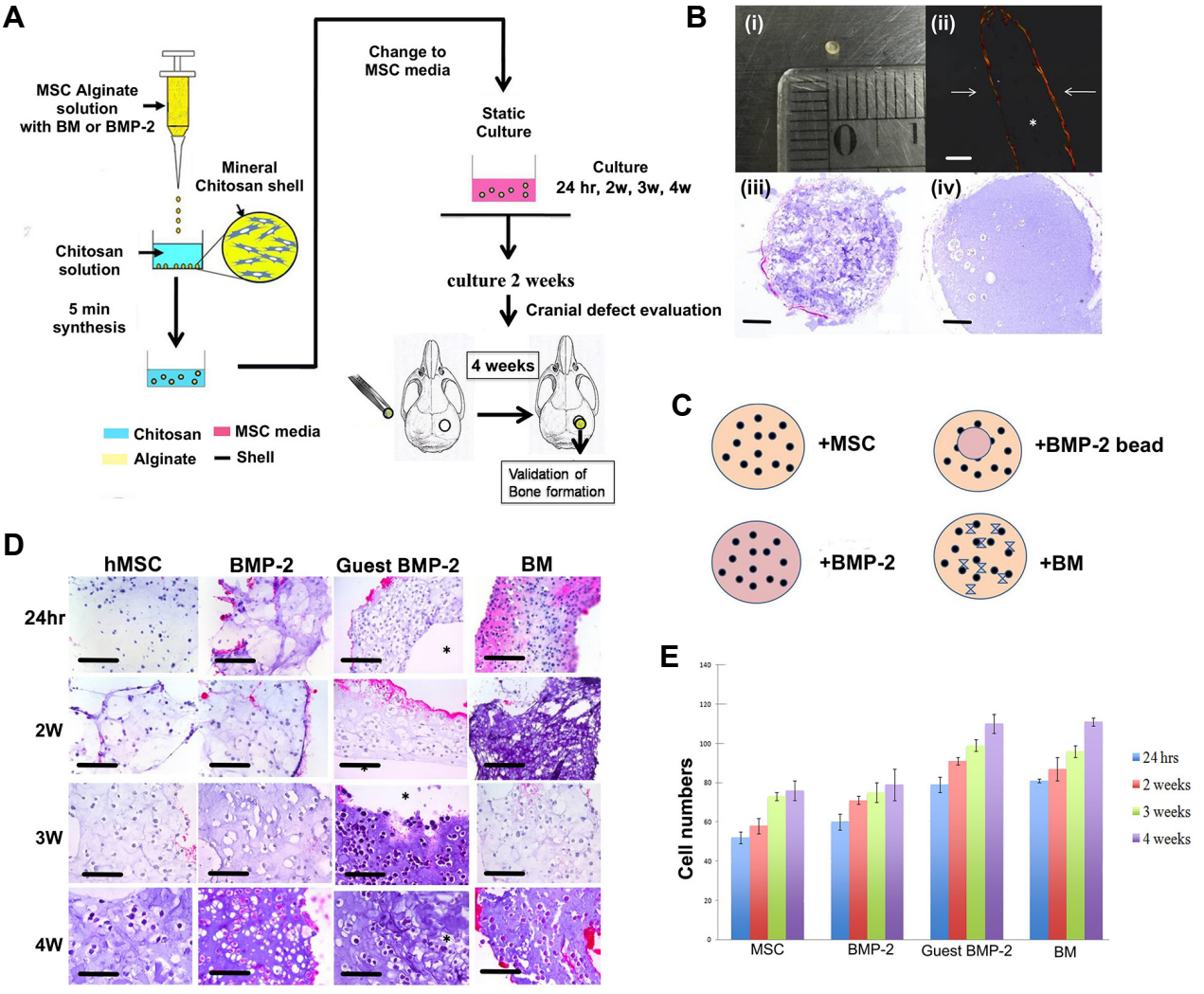

Fig. 1. (A) A schematic diagram detailing the fabrication of the mineralized alginate-chitosan beads and analysis. Mineralized polysaccharide beads were cultured in static or dynamic conditions. Transplanted beads were cultured in static conditions for one day before implantation. In this study, we looked at cell osteoinduction in 3-types of alginate microenvironment differing in ECM components. We compared the effectiveness of BM and BMP-2 in alginate beads to differentiate MSCs into osteogenic cells and osteoid tissue. (B) Standardized bead shape, size, shell structure and internal architecture of alginate beads; (i) Single alginate bead measuring 1 mm in diameter; (ii) light microscope image in polarized light to highlight the semi-crystalline structure of the calcium phosphate/ chitosan shell surrounding the alginate core (white arrow). (iii) Histological thin section of a single bead to demonstrate the internal architecture and external morphology; (iv) a single H & E stained sectioned bead to show the distribution of a fully loaded capsule for cell culture; (C) a diagrammatic representation of the four different types of augmented bead environments used in the study; (D) H&E staining of capsules containing hMSCs at different time points in the four individual bead microenvironments (BMP-2 added, BM proteins added, guest, added and normal alginate) to show the changes in cell distribution, density and proliferation. hMSCs inside BMP-2 beads, guest BMP-2 beads, and BM beads increased cell numbers compared to alginate beads. Also, in control group, hMSCs inside alginate beads distributed well separated and did not form clusters compared experiment groups. (E) hMSC numbers increased significantly in the guest BMP-2 beads and the BM beads compared to the MSCs beads and the BMP-2 beads. (* = Guest BMP-2 bead) (Scale bar = 200 μm).

remodeled the matrix and began changing phenotype from stem to blast (Fig. 1D). By contrast, MSC beads had a more rigid structure without lacunae. At two weeks, hMSCs in BMP-2 beads created chains along the capsule edge and formed small (50-100 μm), close cell clusters. By contrast, hMSCs in standard alginate were well separated and did not form clusters (Fig. 1D). At four weeks, the BMP-2 beads, BM beads, and guest BMP-2 beads generated 150-200 μm spherical cell aggregates.

Analysis of cell phenotype changes in beads

We traced the phenotypic changes in hMSCs encapsulated

inside alginate beads, BMP-2 alginate, and alginate entrapped small ECM proteins, which are vital components of the basement membrane interface. Immuno-based phenotyping was the central method of determining early pathways in bone formation. A primary signaling pathway for bone formation is FGF of which Runx-2 is an essential downstream effector and BMP-related pathways (Maxhimer et al., 2015). The engineered alginate microenvironments drive cell osteogenesis into osteoblast-like cells (Fig. 2A). Moreover, extracellular matrix synthesis from cells was increased by BMP-2 and BM exposure. The nature of the secreted ECM was bone-specific collagen type I. At first encapsulated hMSCs expressed a typical stem cell-related phenotype marker, CD90 over two weeks at variable levels depending on the kind of microenvironment that it was exposed to (Fig. 2A and Supplementary Fig. S1A-S1C). As a result, the fraction of CD90 expressing cells markedly decreased in BMP-2, and ECM infused alginate beads. Therefore, exposure to BMP-2 or ECM proteins removed cell stemness. Thus, it was most likely that the BMP-2 beads converted most CD90 negative cells into osteogenic ones. Osteogenic marker expressions later confirmed the osteogenic nature of the cells.

Next, we analyzed cells according to a selection of critical osteolineage markers, representing the early, mid and late stages of osteogenic lineage conversion. Osterix (Sp7), Runx-2, and osteocalcin were compared by cell counts between the different bead microenvironments: standard alginate without protein encapsulates, and beads individually infused with BMP-2, nested BMP-2 and BM proteins (Figs. 2A and 2B). At the earliest stage of bone cell routing Osterix (Sp7) is expressed. MSCs expressed Osterix in alginate, and in BMP-2 and BM beads at similar levels over two weeks; however, cell expression of Runx-2 was greater inside BMP-2 beads and almost absent from alginate beads. Since Runx-2 is a primary effector in osteogenesis, the BMP-2 induced osteogenic cell fates occurred in the majority of MSCs (Fig. 2B(i)). The minimal hMSC-to-OB conversion observed may be a result of the high quantities of the calcium phosphate present inside the beads. Expression of the CD90 indicator for stemness maintained a high level (75% of total cells) in alginate beads. Whereas, expression of CD90 was non-existent in the BM and BMP-2 infused beads (Fig. 2B(ii)). Cell expression of osteocalcin was more common in BM beads, and this coincided with non-CD90 expressing cells, implying that the vast majority of cells were specialized (Fig. 2B(iii)).

Evaluation of the osteoinductive bead microenvironment on hMSCs

Cell osteoinduction by BMP-2 saturated beads was evaluated by the expression for Runx-2 and Ostecalcin, which are markers of the mature phases of osteogenesis (Figs. 2A and 2B). We used two kinds of BMP-2 engineered bead with individual rates for BMP-2 cell delivery. BMP-2 is a highly mobile small molecule (10 kDa), and its functional-life is short (Caccavo et al., 2018; Green et al., 2005; Utesch et al., 2011). Therefore, BMP-2 rapidly exits the alginate bead in a single burst representing a high percentage of the original BMP-2 quantity. BMP-2 permeability is slowed by the existence of the semi-permeable chitosan-calcium phosphate shell, sustaining levels of BMP-2 for cell differentiation. Cells in alginate do not become osteogenic, and only cells in BMP-2 beads. Depositing a BMP-2 guest into the MSC host bead, where the diffusion of BMP-2 crosses two membranes along the BMP-2 concentration gradient, prolonged delivery. Osteoinductive BMP-2 levels were sustained longer in the MSC beads, and this increased the cell potency of BMP-2. Alizarin red detected positive mineralization in the BMP-2 beads at three weeks (Supplementary Figs. S1A and S1B). Plane-polarized light discovered numerous mineralized nodules inside BMP-2 infused beads and inside BM beads, but not inside MSC beads. Osteocalcin cell expression inside BMP-2 beads was widespread at 14 days and 21 days. We calculated that 79% of counted cells were OCN positive. Cell OCN expression was at 5% in the BMP-2 free alginate (Fig. 2B(iii)).

Evaluation of the basement membrane proteins-infused bead environment on hMSCs

BMP-2 is widely used to induce stem cell differentiation into osteoblasts. Beads infused with 200 ng/ml of BMP-2 rapidly differentiate MSCs into osteocalcin and Runx-2 positive cells and committing the cells to an osteoblast fate. (Fig. 2A, B). Alternatively, BM proteins entrapped in the alginate matrix can provide platforms to fix the MSCs into the tight well-coordinated positions necessary to induce tissue formation responses. In conditions provided by the BM proteins in the microenvironment create certain mechanical and tensional forces on the cell membrane and also within the cytoskeleton, which lead to differentiation and specializations related to the strength of the force fields in the matrix (Engler et al., 2006; Lv et al., 2015).

Besides, stiffness and elasticity are essential properties of the material. Moreover the receptor-integrin interlocking the complex between the polypeptides and cell surface receptors activates vital SMAD related pathways, such as MAPK/ERK into the nucleus (Heldin et al., 1997; Shi et al., 2003). Interestingly, compared with BMP-2 concentration, BM increased osteocalcin expression at three weeks and resulted in increased formation of mineral nodules compared to the BMP-2 beads (Supplementary Figs. S1E and S1F). Furthermore, there was a 10% reduction in stem cells in the BM beads compared to BMP-2 beads (Fig. 2B(iii)).

The performance of hMSC laden beads inside a murine cranial non-union defect

Beads with assorted MSCs, BM proteins and BMP-2 encapsulates regenerated large pockets of osteoid tissue inside a living non-union cranial defect at four weeks. Masson's Trichrome staining, OCN and OPN immunolabelling highlighted the density and distribution of osteoid (Fig. 2C). The BMP-2 alginate beads generated a chain of osteoid pockets across the defect and some of these adequately mineralized (Fig. 2C). However, mineralized tissue was absent from defects bridged by beads without BMP-2 and the BM beads, although BM beads showed the large pockets of osteoid as well. Thus, osteoid tissue generated only in the presence of BMP-2 or BM proteins. The osteoid in the BM and BMP-2 beads strongly stained for Osterix, OCN and OPN (Fig. 2A)

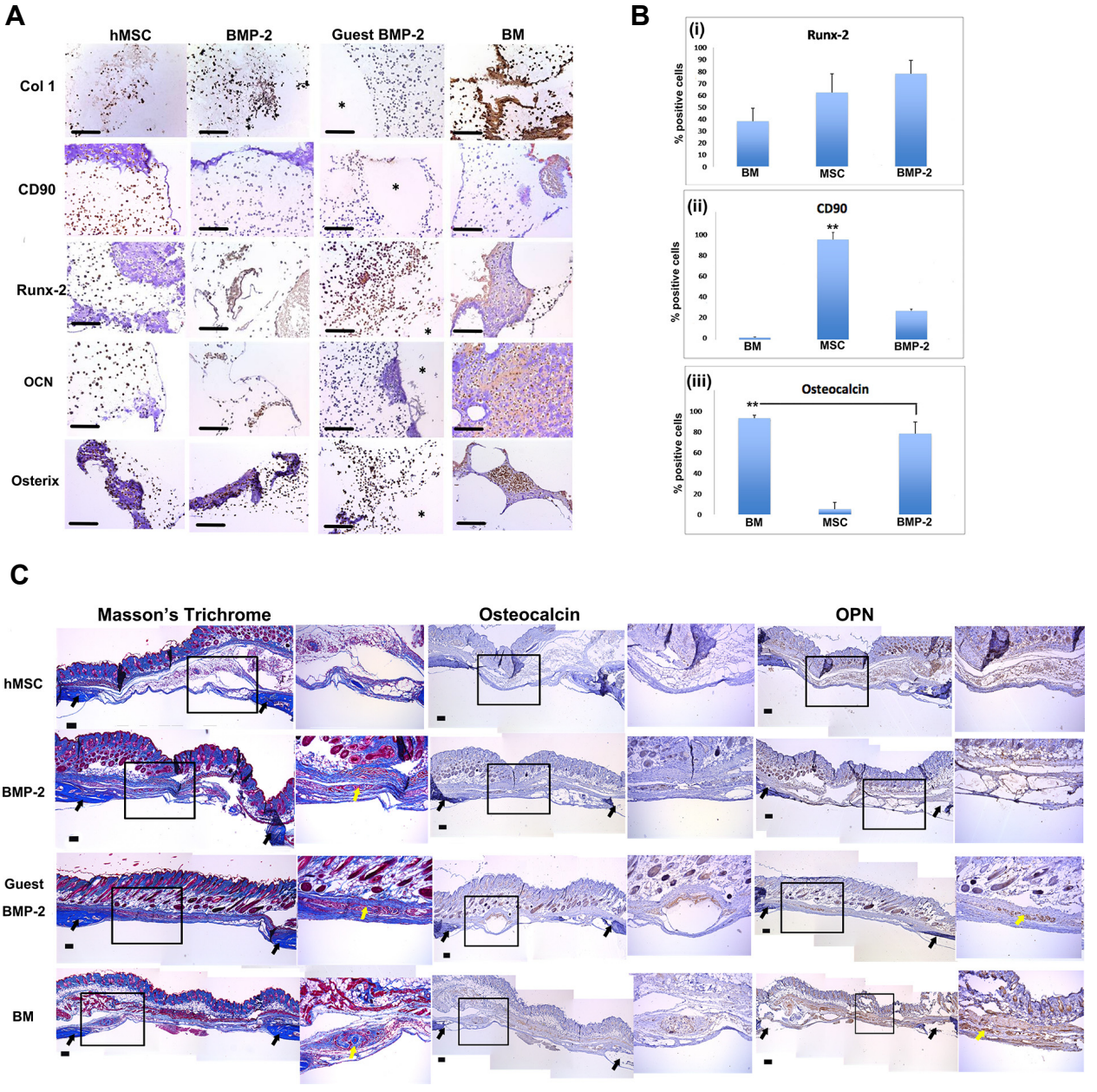

Fig. 2. (A) Immunolabeling results to identify osteogenic related proteins contrasting between the hMSCs beads, BMP-2 beads, guest BMP-2 beads and BM beads. After two weeks culture, collagen I expression was stronger in the BMP-2 added group and BM added group compared to control group and guest BMP-2 group. The CD 90 expression was absent in all groups after two weeks culture. Thus, all encapsulating hMSCs lost stemness after two weeks culture. MSCs expressed Osterix, the marker for pre-osteoblasts, in alginate, and at higher levels in the BMP-2 and BM beads. Runx-2 staining was positive in the BMP-2 added, guest BMP-2 added and the BM beads, and absent in the control group. The osteocalcin cell expression in the BM beads compared with alginate beads, BMP-2 beads and nested BMP-2 beads; (scale bar = 400 μm); (B) percentages of positively versus negatively stained cells for Runx-2, osteocalcin, and CD90 to show the maturation phase of the hMSCs and their conversion into osteogenic lineage cells. (* = Guest BMP-2 bead). (C) Masson's trichrome staining shows the in vivo generated structures from the four different kinds of alginate bead transplants within a mouse cranial bone defect. We find a difference between the MSC control beads inside the defect, and the added BMP-2 and BM alginate beads, which both show a narrowing of the pockets and contain osteoid tissue. More significantly, we see that the beads harboring a BMP-2 guest bead generated an extensive series of osteoid pockets across the defect region (C) accompanied by an even tighter narrowing of the regenerated tissue inside the defect. The IHC staining for OCN and OPN is negative among the control MSC beads. In contrast to the MSC beads, BMP-2 and BM laden beads were OPN and OCN positive. The spaces represent the alginate. Among the defects containing nested alginate beads, the staining for OCN and OPN was larger, more widespread and associated with the osteoid pockets (C; * = Guest BMP-2 bead; black arrows: host bone, yellow areas: newly formed hard tissue) (Scale bar = 200 μm).

moreover mineralization existed in some of the pockets inside defects containing the nested BMP-2 beads. However, mineralization was not widespread, as it usually takes 6-12 weeks for cranial defects to close entirely with new regenerated bone.

DISCUSSION

Soft polysaccharide beads provide a 3D immersive environment for encapsulated hMSCs. Regular alginate is insufficient by itself to initiate differentiation and proliferation of hMSCs at high rates. Therefore, alginate has to be modified and enhanced to stimulate, promote and accelerate proliferation and differentiation. One of the methods to accomplish this is by combining native biological molecules with regenerative effects. For example, the RGD cell adhesive integrin has been conjugated to alginate and shown to increase attachment. Alginate has been modified by sodium periodate to ease degradation. A primary strategy, to accommodate alginate for tissue regeneration, is to infuse alginate with cell-influential ECM proteins, hormones and mobile growth factors. We recreated natural microenvironments in this study for bone tissue formation using a small number of BM proteins and the BMP-2 morphogen. Strongly mineralized was created, which served two purposes: (1) to strengthen the chitosan shell and (2) generate a mineralized background and stimulate bone formation. It was necessary to determine which key components to incorporate the alginate to maximize the bone formation potential while minimizing the types and quantities of encapsulates to use. Thus, we selected human basement membrane proteins (polypeptides), human placenta collagen IV, Laminin and Chondroitin sulfate (CS) to allow biological fixation and ensures orderly cell organization to occur by natural mechanisms. BMP-2 was trapped inside of the alginate pores and adsorbed into the polymer network. BMP-2 is a high potency bone regenerative morphogen that has been used in clinical bone repair with fair success, although slow release into the bone environment is desirable.

Adding BM molecules into the beads accelerated hMSC differentiation into the osteogenic lineage and improved the potential for bone formation than BMP-2 encapsulated beads. Mineral nodules were detected inside beads containing BMP-2 and BM proteins, but with an estimated 10% increase for the BM laden beads. Unadulterated beads merely maintained cells in small clusters with little matrix secretion and remodeling whereas, in ECM beads, tissue formation occurred over large volumes of the bead (25-30% of the total volume capacity). The mineralized beads harbor bone regenerating microenvironments from adult mesenchymal stem cells and can be easily handled and transplanted into bone defects without damage and loss of function. Because the beads are relatively stiff and stable, they may be of clinical use. The mineralized beads transplant therapeutic cells in a microenvironment that is ideal for cell conversion to osteogenic cells, synthesis of bone mineral nodules supported by a bone type collagen I framework. Significant tissue regeneration occurs in beads at a bone non-union defect site. Osteoid tissue forms a sharp line across the defect supported by collagen either side in a short time of four weeks. Beads nested with a BMP-2 guest gave the accelerated 4-week response with signs of mineralization around some of the osteoid pockets distributed along the chain like no other bead type. The osteoid pockets are the foundations for mineral deposition and densification. We may expect widespread mineralization over the osteoid framework at 6 and 12 weeks, which is the typical time for complete bridging of a non-union cranial defect.

Note: Supplementary information is available on the Molecules and Cells website (www.molcells.org).

ACKNOWLEDGEMENTS

This research was supported by a grant of the Korea Health Technology R&D Project through the Korea Health Industry Development Institute (KHIDI), funded by the Ministry of Health & Welfare, Republic of Korea (HI14C1817). This research was financially supported by grants from the National Research Foundation of Korea (NRF) Grant funded by the Korean Government (MSIP) (NRF-2017M3A9B3061833).

REFERENCES

Augst, A.D., Kong, H.J., and Mooney, D.J. (2006). Alginate hydrogels as biomaterials. Macromol. Biosci. *7*, 623-633.

Bouhadir, K.H., Lee, K.Y., Alsberg, E., Damm, K.L., Anderson, K.W., and Mooney, D.J. (2001). Degradation of partially oxidized alginate and its potential application for tissue engineering. Biotechnol. Prog. *17*, 945-950.

Burdick, J.A., Mauck, R.L., and Gerecht, S. (2016). To serve and protect: hydrogels to improve stem cell-based therapies. Cell. Stem. Cell. *18*, 13-15.

Caccavo, D., Cascone, S., Lamberti, G., and Barba, A.A. (2018). Hydrogels: experimental characterization and mathematical modelling of their mechanical and diffusive behaviour. Chem. Soc. Rev. *47*, 2357.

Chaudhuri, O., Koshy, S.T., Branco da Cunha, C., Shin, J.W., Verbeke, C.S., Allison, K.H., and Mooney, D.J. (2014). Extracellular matrix stiffness and composition jointly regulate the induction of malignant phenotypes in mammary epithelium. Nat. Mater. *13*, 970-978.

Collier, J.H., and Segura, T. (2011). Evolving the use of peptides as components of biomaterials. Biomaterials *32*, 4198-4204.

Crane, G.M., Ishaug, S.L., and Mikos, A.G., (1995) Bone tissue engineering. Nat. Med. *1*, 1322-1324.

Fonseca, K.B., Gomes, D.B., Lee, K., Santos, S.G., Sousa, A., Silva, E.A., Mooney, D.J., Granja, P.L., and Barrias, C.C. (2014). Injectable MMP-sensitive alginate hydrogels as hMSC delivery systems. Biomacromolecules *15*, 380-390.

Engler, A.J., Sen, S., Sweeney, H.L., and Discher DE. (2006). Matrix elasticity directs stem cell lineage specification. Cell *126*, 677-689.

Gong, T., Xie, J., Liao, J., Zhang, T., Lin, S., and Lin, Y. (2015). Nanomaterials and bone regeneration. Bone Res. *3*, 15029.

Green, D.W., Leveque, I., Walsh, D., Howard, D., Yang, X.B., Partridge, K.A., Mann, S., and Oreffo, R.O.C. (2005). Biomineralized polysaccharide capsules for encapsulation, organization and delivery of human cell types and growth factors. Adv. Funct. Mater. *15*, 917-923.

Heldin, C.H., Miyazono, K., and ten Dijke, P. (1997). TGF-beta signalling from cell membrane to nucleus through SMAD proteins.

Nature *390*, 465-471.

Jang, K.I., Chung, H.U., Xu, S., Lee, C.H., Luan, H., Jeong, J., Cheng, H., Kim, G.T., Han, S.Y., Lee, J.W., et al. (2015). Soft network composite materials with deterministic and bio-inspired designs. Nat. Commun. *6*, 6566.

Lee, K.Y., and Mooney, D.J. (2012). Alginate: properties and biomedical applications. Prog. Polym. Sci. *37*, 106-126.

Luo, Z., Yang, Y., Deng, Y., Sun, Y., Yang, H., and Wei, S. (2016). Peptide-incorporated 3D porous alginate scaffolds with enhanced osteogenesis for bone tissue engineering. Colloids. Surf. B Biointerfaces *143*, 243-251.

Lv, H., Li, L., Sun, M., Zhang, Y., Chen, L., Rong, Y., and Li, Y. (2005). Mechanism of regulation of stem cell differentiation by matrix stiffness. Stem. Cell Res. Ther. *6*, 103.

Ma, W., Tavakoli, T., Derby, E., Serebryakova, Y., Rao, M.S., and Mattson, M.P. (2008). Cell-extracellular matrix interactions regulate neural differentiation of human embryonic stem cells. BMC Dev. Biol. *8*, 90.

Moshaverinia, A., Ansari, S., Chen, C., Xu, X., Akiyama, K., Snead, M.L., Zadeh, H.H., and Shi, S. (2013). Co-encapsulation of anti-BMP2 monoclonal antibody and mesenchymal stem cells in alginate microspheres for bone tissue engineering. Biomaterials *34*, 6572-6579.

Mao, A.S., Shin, J.W., Utech, S., Wang, H., Uzun, O., Li, W., Cooper, M., Hu, Y., Zhang, L., Weitz, D.A., et al. (2017). Deterministic encapsulation of single cells in thin tunable microgels for niche modelling and therapeutic delivery. Nat. Mater. *16*, 236-243.

Maxhimer, J.B., Bradley, J.P., and Lee, J.C. (2015). Signaling pathways in osteogenesis and osteoclastogenesis: Lessons from cranial sutures and applications to regenerative medicine. Genes. Dis. 2, 57-68.

Murry, C.E., and Keller, G., (2008). Differentiation of embryonic stem cells to clinically relevant populations: lessons from embryonic development. Cell *132*, 661-680.

Muzzarelli, R.A., El Mehtedi, M., Bottegoni, C., Aquili, A., and Gigante, A. (2015). Genipin-crosslinked chitosan gels and scaffolds for tissue engineering and regeneration of cartilage and bone. Mar. Drugs *13*, 7314-7338.

Perez, R.A., Kim, M., Kim, T.H., Kim, J.H., Lee, J.H., Park, J.H., Knowles, J.C., and Kim, H.W. (2014). Utilizing core-shell fibrous collagen-alginate hydrogel cell delivery system for bone tissue engineering. Tissue Eng. Part A *20*, 103-114.

Place, E.S., Rojo, L., Gentleman, E., Sardinha, J.P., and Stevens, M.M. (2011). Strontium- and zinc-alginate hydrogels for bone tissue engineering. Tissue Eng. Part A *17*, 2713-2722.

Pound, J.C., Green, D.W., Chaudhuri, J.B., Mann, S., Roach, H.I., and Oreffo, R.O.C. (2006). Strategies to promote chondrogenesis and osteogenesis from human bone marrow cells and articular chondrocytes encapsulated in polysaccharide templates. Tissue Eng. *12*, 2789-2799.

Rowley, J.A., Madlambayan, G., and Mooney, D.J. (1999). Alginate hydrogels as synthetic extracellular matrix materials. Biomaterials *20*, 45-53.

Sajesh, K.M., Jayakumar, R., Nair, S.V., and Chennazhi, K.P. (2013). Biocompatible conducting chitosan/polypyrrole-alginate composite scaffold for bone tissue engineering. Int. J. Biol. Macromol. *62*, 465-471.

Shah, K. (2013). Encapsulated stem cells for cancer therapy. Biomatter. *3*, pii: e24278.

Shi, Y., and Massagué, J. (2003). Mechanisms of TGF-beta signaling from cell membrane to the nucleus. Cell *113,* 685-700.

Sowjanya, J.A., Singh, J., Mohita, T, Sarvanan, S., Moorthi, A., Srinivasan, N., and Selvamurugan, N. (2013). Biocomposite scaffolds containing chitosan/alginate/nano-silica for bone tissue engineering. Colloids and Surfaces B Biointerfaces *1*, 294-300.

Stevens, M.M. (2008). Biomaterials for bone tissue engineering. Mats. Today *11*, 18-25.

Swioklo, S., Constantinescu, A., and Connon, C.J. (2016). Alginate-encapsulation for the improved hypothermic preservation of human adipose-derived stem cells. Stem. Cells Transl. Med. *5*, 339-349.

Xia, Y., Mei, F., Duan, Y., Gao, Y., Xiong, Z., Zhang, T., and Zhang, H. (2013). Bone tissue engineering using bone marrow stromal cells and an injectable sodium alginate/gelatin scaffold. Journal of Biomedical Materials Research Part A. *109*, 294-300.

Yang, X.B., Whitaker, M.J., Sebald, W., Clarke, N., Howdle, S.M., Shakesheff, K.M., and Oreffo. R.O. (2004). Human osteoprogenitor bone formation using encapsulated bone morphogenetic protein 2 in porous polymer scaffolds. Tissue Eng. *10*, 1037-1045.